

## Large muon ( $g - 2$ ) from TeV-scale MSSM with infinite $\tan\beta$

---

**Jae-hyeon Park\***

*Departament de Física Teòrica and IFIC, Universitat de València-CSIC, 46100, Burjassot, Spain*

*E-mail: jae.park@uv.es*

**Markus Bach, Dominik Stöckinger and Hyejung Stöckinger-Kim**

*Institut für Kern- und Teilchenphysik, TU Dresden, 01069 Dresden, Germany*

*E-mail: markus.bach1@tu-dresden.de, dominik.stoeckinger@tu-dresden.de,  
hyejung.stoeckinger-kim@tu-dresden.de*

The muon anomalous magnetic moment  $a_\mu$  is studied in the infinite  $\tan\beta$  limit of the MSSM. Since the muon mass arises completely from loop effects, large corrections to  $a_\mu$  are expected in comparison to the usual case with moderately high  $\tan\beta$ . Due to the qualitatively different parameter dependence, the gap between the experimental value and the Standard Model prediction can be filled only in parameter volumes in which a mass hierarchy suppresses the chargino loop in favour of the neutralino contribution. Two such possibilities are found to have either large Higgsino mass or large muon sneutrino mass. Supersymmetric particles even at the TeV scale can lead to the best fit of  $a_\mu$ .

*18th International Conference From the Planck Scale to the Electroweak Scale  
25-29 May 2015  
Ioannina, Greece*

---

\*Speaker.

The muon anomalous magnetic moment,  $a_\mu \equiv (g_\mu - 2)/2$ , has long been a prime observable sensitive to hypothetical virtual states, and hence a major indirect probe to new physics. Currently, there is an interesting discrepancy between the experimental and the Standard Model (SM) values of  $a_\mu$  [1]:

$$a_\mu^{\text{exp}} - a_\mu^{\text{SM}} = (28.7 \pm 8.0) \times 10^{-10}, \quad (1)$$

which amounts to more than  $3\sigma$ . This has called for many attempts to fill the gap with various new physics contributions.

In this respect, one noteworthy property of  $a_\mu$  is that it is correlated with loop corrections to the muon mass  $m_\mu$ . This is easy to see by comparing the schematic diagrams of  $a_\mu$  and the muon self energy  $\Sigma_\mu$ , shown in figure 1. Manifestly, attaching a photon line to the  $\Sigma_\mu$  graph on the right

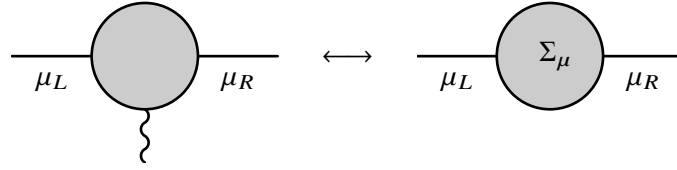


Figure 1: Diagrammatic similarity between  $a_\mu$  (left) and the muon self energy (right).

results in the  $a_\mu$  diagram on the left. This means that large loop corrections to  $m_\mu$  generically imply large contributions to  $a_\mu$ .

For this reason, there have been significant interests in models where  $m_\mu$  arises solely from loop effects. This idea may be realized for instance within a popular model such as the minimal supersymmetric standard model (MSSM). In this model, the tree-level muon mass is given by

$$m_\mu^{\text{tree}} = y_\mu v_d, \quad (2)$$

the product of  $y_\mu$ , the muon Yukawa coupling, and  $v_d$ , the vacuum expectation value (VEV) of the down-type Higgs. Obviously, this leads to the following two options to eliminate the tree-level muon mass: (a)  $y_\mu = 0$  or (b)  $v_d = 0$ . There are already studies which employ the former approach while using the non-holomorphic [2] or the holomorphic [3] smuon trilinear coupling for the radiative generation of  $m_\mu$ . We consider the latter option focusing on the supersymmetric contributions to  $a_\mu$  [4] which shall be the subject of this presentation.

The supersymmetric contributions to  $a_\mu$  at the one-loop level are well-known in the MSSM [5]. They arise from the chargino-sneutrino and the neutralino-smuon diagrams which depend on the following five mass parameters: the Higgsino mass  $\mu$ , the bino mass  $M_1$ , the wino mass  $M_2$  as well as the soft masses of the left- and the right-handed smuons,  $m_L$  and  $m_R$ . In a simplified case where all these five parameters are equal to  $M_{\text{SUSY}}$ , the above contributions can be approximated by

$$a_\mu^{\text{SUSY,1L}} \approx 13 \times 10^{-10} \text{ sign}(\mu) \tan\beta \left( \frac{100 \text{ GeV}}{M_{\text{SUSY}}} \right)^2. \quad (3)$$

One can notice the following properties of  $a_\mu^{\text{SUSY,1L}}$ : (a) it is suppressed by the second power of  $M_{\text{SUSY}}$ , the new physics scale, (b) it is proportional to  $\tan\beta$ , (c) its sign is determined by the sign

of  $\mu$ . For a usual value of  $\tan\beta \lesssim 60$ , the best fit of (1) is achieved only if  $M_{\text{SUSY}} \lesssim 500$  GeV. Now that the Large Hadron Collider is putting more and more stringent lower bounds on the supersymmetric particle masses, one may consider how to fit (1) even for higher  $M_{\text{SUSY}}$ .

To this end, a straightforward attempt would be to push  $\tan\beta$  up beyond the usual range. This has been however a less explored possibility. The fear is mostly based on the perturbativity of the down-type Yukawa couplings. As they are proportional to  $\tan\beta$  under the tree-level approximation, one might naively expect them to grow nonperturbatively large for too high  $\tan\beta$ . It is however well-known that the down-type fermion masses can receive significant loop corrections which pick up the up-type Higgs VEV  $v_u$  [6]. This effect may be expressed in the form,

$$m_f = y_f v_d + y_f v_u \Delta_f^{\text{red}}, \quad (4)$$

where  $m_f$  is the pole mass of  $f$  standing for a charged lepton or down-type quark,  $y_f$  is its Yukawa coupling, and  $\Delta_f^{\text{red}}$  is a finite quantity calculable from the self energy diagrams. This implies that  $m_f$  might be correct even if  $v_d$  is unconventionally small or even vanishes. Indeed, it has been shown that such a possibility can meet various phenomenological constraints [7, 8].

With  $\Delta_f^{\text{red}}$  from (4) taken into account, the supersymmetric contribution to  $a_\mu$  becomes [9]

$$a_\mu^{\text{SUSY}} = \frac{a_\mu^{\text{SUSY,1L}}}{1 + \tan\beta \Delta_\mu^{\text{red}}} \equiv \frac{y_\mu v_u}{m_\mu} a_\mu^{\text{red}}, \quad (5)$$

where  $a_\mu^{\text{SUSY,1L}}$ , appearing on the left-hand side of (3), is the supersymmetric one-loop contribution to  $a_\mu$  without resummation of  $\tan\beta$ -enhanced terms. One can understand the first equality above in the following way. Due to the chiral symmetry, both  $a_\mu^{\text{SUSY}}$  and  $a_\mu^{\text{SUSY,1L}}$  contain a factor of  $y_\mu$  which is rewritten in terms of the other quantities appearing in (4). This replacement is done however to differing accuracies, i.e. the  $\Delta_f^{\text{red}}$  term in (4) is neglected for  $a_\mu^{\text{SUSY,1L}}$  whereas it is included for  $a_\mu^{\text{SUSY}}$ . The above resummation formula then follows. Another quantity  $a_\mu^{\text{red}}$  is defined in (5), in terms of which the infinite  $\tan\beta$  limit of  $a_\mu^{\text{SUSY}}$  reads simply

$$\lim_{\tan\beta \rightarrow \infty} a_\mu^{\text{SUSY}} = \frac{a_\mu^{\text{red}}}{\Delta_\mu^{\text{red}}}, \quad (6)$$

which follows from (4) and (5).

In this limit, one can again consider a simplified case where the five mass parameters are the same to obtain an expression analogous to (3). This results in

$$\lim_{\tan\beta \rightarrow \infty} a_\mu^{\text{SUSY}} \approx -72 \times 10^{-10} \left( \frac{1 \text{ TeV}}{M_{\text{SUSY}}} \right)^2. \quad (7)$$

For the same new physics scale  $M_{\text{SUSY}}$ , the magnitude of  $a_\mu^{\text{SUSY}}$  above does greatly exceed that of (3) valid for moderate  $\tan\beta$ . Unfortunately, the sign turns out to be wrong which, being independent of the  $\mu$  sign, seems unfixable. This is because the diagrams of both  $a_\mu^{\text{red}}$  and  $\Delta_\mu^{\text{red}}$  pick up a Higgsino mass due to the Peccei-Quinn symmetry and therefore the  $\mu$  sign cancels out of (6).

It is still early to give up. One can get a hint on how to overcome this sign problem by closer inspection of the structures of  $a_\mu^{\text{red}}$  and  $\Delta_\mu^{\text{red}}$  appearing in the fraction of (6). Schematically, the

contributions to the numerator and the denominator look like

$$\lim_{\tan\beta \rightarrow \infty} a_\mu^{\text{SUSY}} = \frac{a_\mu^{\text{red}}}{\Delta_\mu^{\text{red}}} \sim \frac{+(\chi^\pm \text{ term}) + (\chi^0 \text{ terms})}{-(\chi^\pm \text{ term}) + (\chi^0 \text{ terms})}, \quad (8)$$

i.e. both  $a_\mu^{\text{red}}$  and  $\Delta_\mu^{\text{red}}$  consist of the chargino terms and the neutralino terms whose diagrams are shown in figure 2 in the mass insertion approximation. The last fraction above is intended

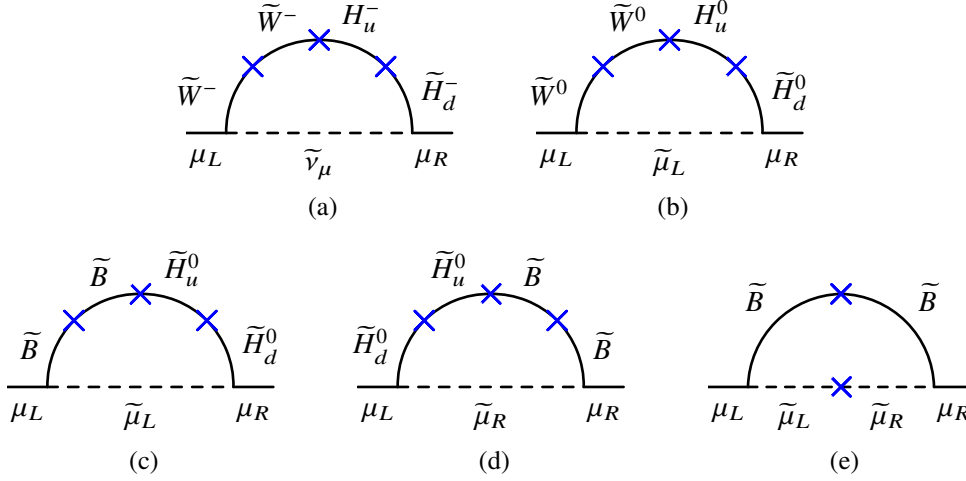


Figure 2: Mass-insertion diagrams for  $\Delta_\mu^{\text{red}}$  and  $a_\mu^{\text{red}}$ . For the latter, an external photon couples to any of the charged particles in the loop.

to mean that the numerical values of the chargino terms in  $a_\mu^{\text{red}}$  and  $\Delta_\mu^{\text{red}}$  have opposite signs to each other whereas the neutralino terms have the same sign. When the five mass parameters are of similar sizes, the chargino terms tend to dominate in both  $a_\mu^{\text{red}}$  and  $\Delta_\mu^{\text{red}}$  thereby resulting in negative  $a_\mu^{\text{SUSY}}$ . A way to turn around the sign would then be to let the neutralino terms dominate or equivalently to suppress the chargino terms in both  $a_\mu^{\text{red}}$  and  $\Delta_\mu^{\text{red}}$ . For this, one may suppress any of the propagators forming the loop of the chargino graph in figure 2(a), as long as some of the neutralino diagrams survive. This leads to the following three solutions: (a) “large- $\mu$  limit” which suppresses the Higgsino propagators as shown in figure 3 while leaving diagram 3(e) unsuppressed, (b) “ $\tilde{\mu}_R$ -dominance” which suppresses the sneutrino propagator by raising  $m_L$  as shown in figure 4 while maintaining the contribution from figure 4(d), (c) suppression of the wino propagators as in figure 5 [as well as the  $\tilde{\mu}_R$  propagators to isolate diagram 5(c)] by raising  $|M_2|$  and  $m_R$ . It turns out that solution (c) requires extreme mass hierarchies to work in practice and is therefore less interesting than the other two options.

As explained above,  $a_\mu^{\text{SUSY}}$  is invariant under a  $\mu$  sign flip. Furthermore, a simultaneous sign flip of both  $M_1$  and  $M_2$  leaves  $a_\mu^{\text{SUSY}}$  in (6) invariant, as one can understand from each diagram in figure 2 which picks up the sign of either  $M_1$  or  $M_2$ . Taking advantage of these symmetries, we shall assume in what follows that  $\mu$  and  $M_1$  are positive without loss of generality while leaving the  $M_2$  sign free.

With the above qualitative observations in mind, one can examine in more detail how the sign of  $a_\mu^{\text{SUSY}}$  depends on the mass parameters. Two plots are shown in figure 6 employing the mass insertion approximation under which the sign of  $a_\mu^{\text{SUSY}}$  is fully determined by the ratios of the

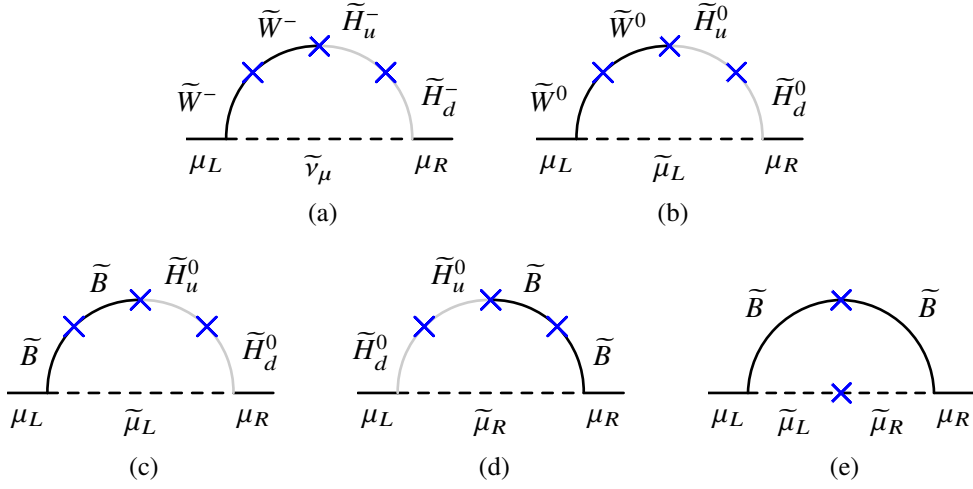


Figure 3: Same diagrams as in figure 2 in the “large- $\mu$  limit”. Grey lines represent mass-suppressed propagators.

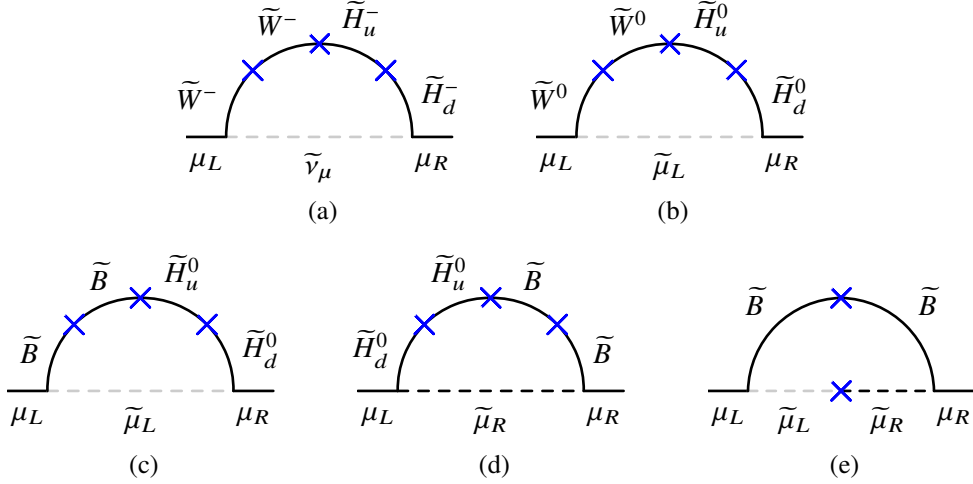


Figure 4: Same diagrams as in figure 2 in the case of “ $\tilde{\mu}_R$ -dominance”. Grey lines represent mass-suppressed propagators.

five mass parameters. In figure 6(a), the origin at which the mass parameters are equal leads to negative  $a_\mu^{\text{SUSY}}$  as already seen in (7). In the same plot, one finds indeed the two types of regions where  $a_\mu^{\text{SUSY}}$  is positive as expected from the aforementioned mass hierarchies: the white regions on the right and around the upper border correspond to the “large- $\mu$  limit” and “ $\tilde{\mu}_R$ -dominance”, respectively. The less interesting solution (c) is visible as a small white area around the left part of the bottom border of figure 6(b), in which  $|M_2|$  and  $m_R$  are much larger than the other three mass parameters.

Given a set of the mass parameter ratios leading to the desired sign of  $a_\mu^{\text{SUSY}}$ , its size can be adjusted to fit (1) by choosing an overall mass scale. Obviously, the higher the mass scale is, the smaller  $a_\mu^{\text{SUSY}}$  becomes. We parametrize the scale by  $M_{\text{SUSY},\text{min}}$ , the smallest of  $\{\mu, M_1, |M_2|, m_L, m_R\}$ . The results are presented in figure 7 in which one finds regions with colours corresponding to

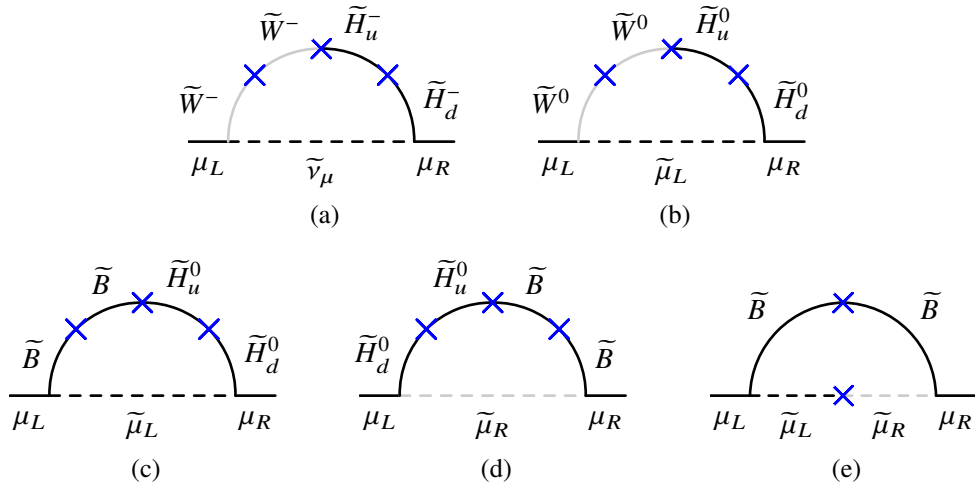


Figure 5: Same diagrams as in figure 2 in the case where  $M_1, \mu, m_L \ll |M_2|, m_R$ . Grey lines represent mass-suppressed propagators.

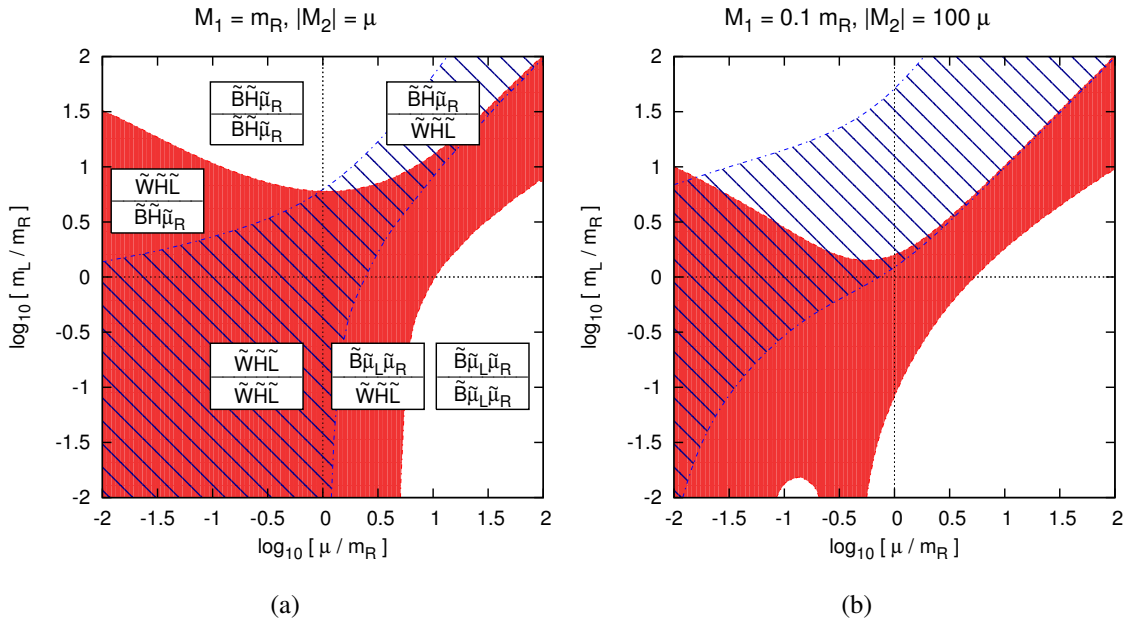


Figure 6: Sign of  $a_\mu^{\text{SUSY}}$  on the plane of  $(\mu/m_R, m_L/m_R)$  for the two signs of  $M_2$ . The remaining two mass ratios are fixed as shown above each plot. The sign of  $a_\mu^{\text{SUSY}}$  in each region is: + in white,  $\text{sign}(-M_2)$  in red,  $\text{sign}(+M_2)$  in hatched, - in overlap.

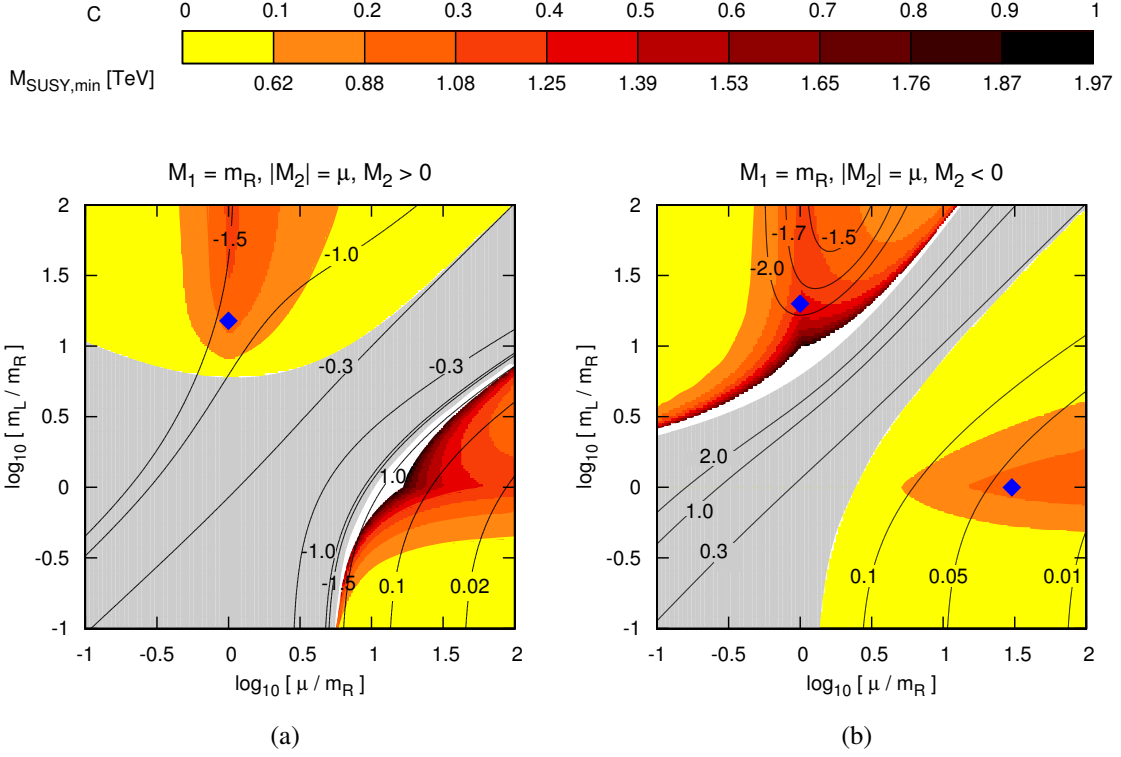


Figure 7: Values of  $M_{\text{SUSY,min}}$  for the best fit of  $a_\mu^{\text{SUSY}}$  are represented on the plane of  $(\mu/m_R, m_L/m_R)$  as the gradation of colour, for (a) positive and (b) negative  $M_2$ . The grey regions lead to negative  $a_\mu^{\text{SUSY}}$ . The contour lines indicate  $y_\mu$ . In the white regions,  $|y_\mu|$  is nonperturbatively large. The blue diamonds are the specimen points from table 1.

$M_{\text{SUSY,min}}$  around 1 TeV or higher. This reveals a promising possibility that supersymmetric particles at the TeV-scale or higher can explain (1), which is the motivation to consider the infinite  $\tan\beta$  limit in this work.

For this scenario to be viable, it must meet all relevant constraints. The lepton flavour violating process  $\mu \rightarrow e\gamma$  can be suppressed by assuming small enough slepton mixing between the first two generations. The correlation between  $\mu \rightarrow e\gamma$  and  $a_\mu$  [10] still holds for  $\tan\beta \rightarrow \infty$ . One can also satisfy  $B$ -physics constraints [8]. The most dangerous decay mode is  $B^+ \rightarrow \tau^+\nu$  to which the charged Higgs exchange contribution can be suppressed enough by raising  $M_{H^\pm}$  to a few TeV. Pollution to  $B_s \rightarrow \mu^+\mu^-$  and  $B \rightarrow X_s \gamma$  can be suppressed with vanishing  $A_t$  and flavour-violating squark mass insertions. For the former and the latter processes, it further helps to raise the heavy Higgs and the squark masses, respectively. One can make the lightest Higgs mass and decays SM-like by staying in the decoupling regime [11].

Moreover, we impose the following constraints: (a) charginos and smuons are heavier than 100 GeV, (b)  $y_\mu$  is perturbative, (c) our vacuum is stable or long-lived on the cosmological time-scale. To evaluate the false vacuum lifetime, we use the method from ref. [12]. Each of these requirements excludes some regions depicted in figure 8. The plots show that great parts of the “large- $\mu$ ” region for negative  $M_2$  as well as the “ $\tilde{\mu}_R$ -dominance” region for either sign of  $M_2$

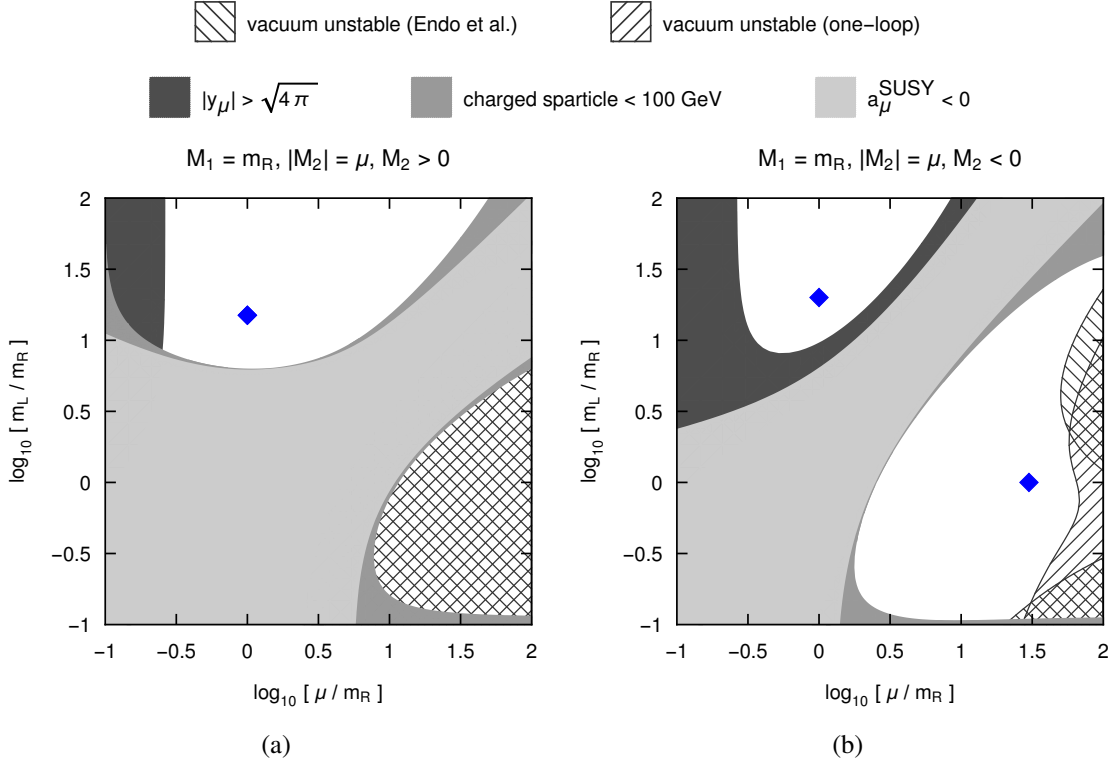


Figure 8: Regions on the plane of  $(\mu/m_R, m_L/m_R)$  excluded by the constraints indicated in the legend, for (a) positive and (b) negative  $M_2$ . The blue diamonds are the specimen points from table 1.

survive the constraints. This means that there are indeed parameter volumes in which TeV-scale supersymmetric particles can account for the measured value of  $a_\mu$ . We also check that  $y_\tau$  and  $y_b$ , the tau and the bottom Yukawas, can be perturbative and consistent with the vacuum metastability. Even though  $m_\tau$ , bigger than  $m_\mu$ , might cause a worry about too large  $|y_\tau|$ , there is room for perturbative radiative generation of  $m_\tau$  since  $(g_\tau - 2)$  does not need to be explained. The even larger bottom quark pole mass can also be perturbatively generated thanks to the gluino-loop contribution in addition to the other types of loops shared by the tau self energy.

The concrete values of the five mass parameters at selected points from figures 7 and 8 are listed in table 1. The first two points belong to the “large- $\mu$  limit” with negative  $M_2$ , and the rest to the “ $\tilde{\mu}_R$ -dominance” regime with either sign of  $M_2$ .

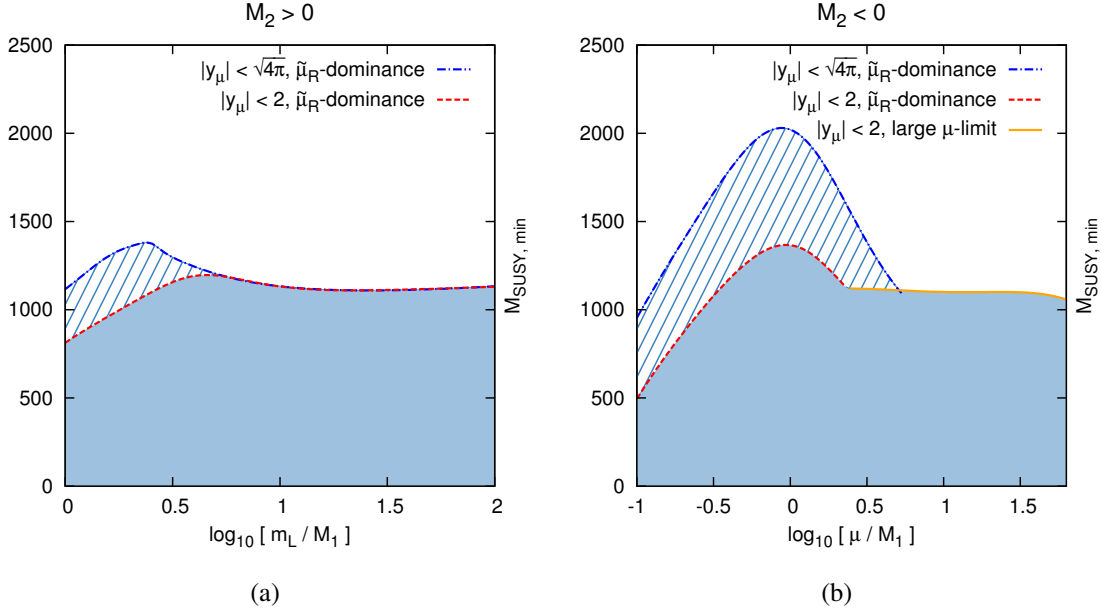
To find maximal  $M_{\text{SUSY}, \min}$  which can fit  $a_\mu$ , we explore the full five-dimensional parameter space, relaxing the equalities,  $M_1 = m_R$  and  $|M_2| = \mu$ , which we assumed for the sake of planar presentation of the preceding plots. The resulting maximum  $M_{\text{SUSY}, \min}$  is plotted in figure 9. The plots reveal that the relaxation of the above mass equalities allows  $M_{\text{SUSY}, \min}$  to be slightly higher than before.

For a compact summary, we derive a formula resembling (7),

$$a_\mu^{\text{SUSY}} \approx 37 \times 10^{-10} \left( \frac{1 \text{ TeV}}{M_{\text{SUSY}}} \right)^2, \quad (9)$$



$\mu$	$M_1$	$M_2$	$m_L$	$m_R$	$a_\mu^{\text{SUSY}}/10^{-9}$	$y_\mu$	Characteristic
30	1	-30	1	1	2.80	0.04	large- $\mu$
15	1	-1	1	1	3.01	0.09	large- $\mu$
1	1	1	15	1	2.64	-1.37	$\tilde{\mu}_R$ -dominance
1	1	30	30	1	2.77	-1.18	$\tilde{\mu}_R$ -dominance
1.3	1.3	-1.3	26	1.3	2.90	-1.89	$\tilde{\mu}_R$ -dominance

Table 1: Specimen points leading to a reasonable fit of  $a_\mu$ . Masses are in TeV.Figure 9: Maximum  $M_{\text{SUSY},\text{min}}$  that can fit  $a_\mu$  as a function of (a)  $m_L/M_1$  for  $M_2 > 0$  and (b)  $\mu/M_1$  for  $M_2 < 0$ . Each line style indicates to which regime the point belongs as well as the cutoff on  $|y_\mu|$ . The vacuum metastability is required.

which applies if either  $|\mu| \gg |M_1| = m_L = m_R \equiv M_{\text{SUSY}}$  or  $m_L \gg |\mu| = |M_1| = m_R \equiv M_{\text{SUSY}}$ . These are two mass hierarchies representative of the “large- $\mu$  limit” and the “ $\tilde{\mu}_R$ -dominance”, respectively.

In summary, we considered the infinite  $\tan\beta$  limit of the MSSM as a possibility to account for the discrepancy between the experimental value and the SM prediction of  $a_\mu$  even if the supersymmetric particles are as heavy as 1 TeV or higher. The motivation was the observation that fully radiative muon mass generation would imply large new physics effects on  $a_\mu$ . We found two successful types of mass hierarchies, the “large- $\mu$  limit”, and the “ $\tilde{\mu}_R$ -dominance”, which allowed us to achieve the goal. We took into account phenomenological constraints from collider searches, flavour and Higgs physics, as well as theoretical constraints from perturbativity and vacuum metastability. For more details of the analysis, we refer the reader to ref. [4].

For those  $a_\mu$  enthusiasts, we add a note on GM2Calc, a calculator of the MSSM contributions

to  $a_\mu$  [13]. It can approximate the infinite  $\tan\beta$  limit as it works for arbitrarily high  $\tan\beta$ .

J.P. acknowledges support from the MEC and FEDER (EC) Grant FPA2011–23596 and the Generalitat Valenciana under Grant PROMETEOII/2013/017.

## References

- [1] M. Davier, A. Hoecker, B. Malaescu and Z. Zhang, *Reevaluation of the Hadronic Contributions to the Muon ( $g - 2$ ) and to  $\alpha(M_Z)$* , *Eur. Phys. J. C* **71** (2011) 1515 [Erratum *ibid.* **C 72** (2012) 1874] [arXiv:1010.4180].
- [2] F. Borzumati, G. R. Farrar, N. Polonsky and S. D. Thomas, *Soft Yukawa couplings in supersymmetric theories*, *Nucl. Phys. B* **555** (1999) 53 [hep-ph/9902443]; A. Crivellin, J. Girrbach and U. Nierste, *Yukawa coupling and anomalous magnetic moment of the muon: an update for the LHC era*, *Phys. Rev. D* **83** (2011) 055009 [arXiv:1010.4485].
- [3] A. Thalappilil and S. Thomas, *Higgs Boson Yukawa Form Factors from Supersymmetric Radiative Fermion Masses*, arXiv:1411.7362.
- [4] M. Bach, J.-h. Park, D. Stöckinger and H. Stöckinger-Kim, *Large muon ( $g - 2$ ) with TeV-scale SUSY masses for  $\tan\beta \rightarrow \infty$* , *JHEP* **1510** (2015) 026 [arXiv:1504.05500].
- [5] T. Moroi, *The Muon anomalous magnetic dipole moment in the minimal supersymmetric standard model*, *Phys. Rev. D* **53** (1996) 6565 [Erratum *ibid.* **D 56** (1997) 4424] [hep-ph/9512396].
- [6] L. J. Hall, R. Rattazzi and U. Sarid, *The Top quark mass in supersymmetric SO(10) unification*, *Phys. Rev. D* **50** (1994) 7048 [hep-ph/9306309].
- [7] B. A. Dobrescu and P. J. Fox, *Uplifted supersymmetric Higgs region*, *Eur. Phys. J. C* **70** (2010) 263 [arXiv:1001.3147].
- [8] W. Altmannshofer and D. M. Straub, *Viability of MSSM scenarios at very large  $\tan\beta$* , *JHEP* **1009** (2010) 078 [arXiv:1004.1993].
- [9] S. Marchetti, S. Mertens, U. Nierste and D. Stöckinger,  *$\tan\beta$ -enhanced supersymmetric corrections to the anomalous magnetic moment of the muon*, *Phys. Rev. D* **79** (2009) 013010 [arXiv:0808.1530].
- [10] J. Kersten, J.-h. Park, D. Stöckinger and L. Velasco-Sevilla, *Understanding the correlation between  $(g - 2)_\mu$  and  $\mu \rightarrow e\gamma$  in the MSSM*, *JHEP* **1408** (2014) 118 [arXiv:1405.2972].
- [11] J. F. Gunion and H. E. Haber, *The CP conserving two Higgs doublet model: The Approach to the decoupling limit*, *Phys. Rev. D* **67** (2003) 075019 [hep-ph/0207010].
- [12] J.-h. Park, *Constrained potential method for false vacuum decays*, *JCAP* **1102** (2011) 023 [arXiv:1011.4936]; *Metastability bounds on flavor-violating trilinear soft terms in the MSSM*, *Phys. Rev. D* **83** (2011) 055015 [arXiv:1011.4939].
- [13] P. Athron, M. Bach, H. G. Fargnoli, C. Gnendiger, R. Greifenhagen, J.-h. Park, S. Paßehr, D. Stöckinger, H. Stöckinger-Kim, A. Voigt, *GM2Calc: Accurate MSSM prediction for  $(g - 2)$  of the muon*, <http://gm2calc.hepforge.org>.